Materials and Structures (2021) 54:61
https://doi.org/10.1617/s11527-021-01643-8

ORIGINAL ARTICLE

The square root method for chloride ingress prediction—Applicability and limitations

Simon Fjendbo · Henrik E. Sørensen · Klaartje De Weerdt · Mette R. Geiker

Received: 2 October 2020 / Accepted: 31 January 2021 / Published online: 4 March 2021

Abstract A recent observation showed a square root time dependency of the ingress depth of a fixed (reference) chloride concentration of 0.05% chloride by mass of concrete for submerged exposure in Kattegat and the Baltic Sea. The purpose of this paper is to assess the applicability and limitations of the observation, widen the scope of validity and propose it as a method. Field data from submerged, tidal, splash, atmospheric and inland deicing salt exposure at various geographical locations was analyzed at a range of reference concentrations. In total 237 combinations of concrete, exposure, and reference concentration were analyzed. Our results showed that chloride ingress of a reference concentration followed a linear relationship with an average R^2 of 0.96, when the penetration depth of the reference concentration was plotted against the square root of the exposure time. The square root observation appeared valid for the studied Portland cement based concretes with fly ash, silica fume and ground granulated blast furnace slag exposed in submerged and tidal exposure zones, when applying reference concentrations of 0.1–1.8% chloride by mass of binder, and reference concentrations of 0.1–0.5% chloride by mass of binder in atmospheric exposure zone. It was found that the parameters describing the straight line depended on the chosen reference concentration and concrete composition, and that the slope of the straight line (ingress parameter) in addition depended on the exposure. It was concluded that the square root method appears to be a promising method for predicting further chloride ingress into concrete.

Keywords Concrete · Chloride ingress · Diffusion · Field exposure · Service life prediction

1 Introduction

It is of increasing importance to predict the long-term chloride ingress in concrete as ever longer design service life requirements are prescribed. Roughly, two types of models for chloride ingress prediction exists: empirical and physical. Empirical models are widely used by engineers in practical applications, which is probably due to their simplicity relative to physical models. Physical models seek to model chloride ingress by e.g. including free chloride as driving

Supplementary Information The online version contains supplementary material available at https://doi.org/10.1617/s11527-021-01643-8.

S. Fjendbo (✉) · H. E. Sørensen
Danish Technological Institute, Taastrup, Denmark
e-mail: simon.fjendbo@ntnu.no

S. Fjendbo · K. De Weerdt · M. R. Geiker
Department of Structural Engineering, Norwegian University of Science and Technology (NTNU), Trondheim, Norway

force, chloride binding, additional transport processes besides diffusion, multi-ionic characteristics, moisture and dissolution/precipitation reactions [1–3].

Empirical chloride ingress models generally require fewer input parameters. Commonly chloride ingress is modeled by the error function solution to Fick's 2nd law of diffusion for a semi-infinite medium. The total chloride content is often considered as the driving force, although only free chloride is available for diffusion [4–7]. To account for the observed decrease of the diffusion coefficient over time, often ingress prediction models include an ageing function [1, 4–11]. A drawback of the ageing function is that it causes the chloride ingress to stop at infinite age (the diffusion coefficient goes towards zero). To avoid this issue, the service life model Life 365 keeps the apparent chloride diffusion coefficient (D_a) constant after 25 years exposure [12]. The surface concentration (C_s) is constant in many models, although it has been observed to increase over time. The HETEK model takes this into account by a time dependent surface concentration [8] based on work by Mejlbro [11]. Finally, the maximum concentration is often observed at a certain depth; either due to convection (as accounted for in e.g. [4]) or due to elemental zonation and leaching [13, 14], which is currently only accounted for by omitting the outer measuring point(s) when fitting data [4].

Another empirical approach to predict chloride ingress could be to follow the ingress of a chloride concentration of interest (e.g. the critical chloride content) rather than the entire chloride profile. Poulsen and Sørensen [15] observed a linear relationship between a reference concentration of 0.05% chloride by mass of concrete and the square root of time and termed this the "square root observation". Poulsen et al. [16] showed an excellent correlation with experimental data of up to 20 years for submerged exposure in Träslövsläge Field Exposure Site in Kattegat and up to five years for submerged exposure at Fehmarn Belt Exposure Site.

According to Poulsen et al. [16] the ingress depth of a reference concentration of 0.05% chloride by mass of concrete ($x_{0.05}$) can for their data be described by Eq. (1).

$$x_{0.05}(t) = a_{0.05} \times \sqrt{t} + b_{0.05} \quad (1)$$

where $a_{0.05}$ is the slope of a straight line, when $x_{0.05}$ is plotted against the square root of exposure time, and $b_{0.05}$ is the intercept. Poulsen et al. [16] interpreted $a_{0.05}$ as an indicator for the long-term chloride penetration rate of the reference concentration (C_r = 0.05% chloride by mass of concrete), while $b_{0.05}$ is interpreted as an indicator for the ingress relatively faster than $a_{0.05}$ occurring at early age. Hereafter the slope of the straight line for a C_r is mentioned as a_{Cr} (ingress parameter), the intercept as b_{Cr} (early ingress depth), and the ingress depth as x_{Cr}.

In the square root observation, the ingress parameter is constant with square root of exposure time and the challenge of the chloride ingress approaching zero exponentially for long term exposure is thereby overcome. However, the analysis by Poulsen et al. [16] only applied the square root method on data from submerged exposure at Fehmarn Belt and Träslövsläge Exposure Sites and only for a reference concentration of 0.05% chloride by mass of concrete.

Covering other types of exposure (wetting and drying), Thomas and Matthews [17] plotted the depth of penetration of 0.4% chloride by mass of binder versus the square root of exposure time for concrete with water-to-cement ratio (by mass) (w/c) 0.37–0.57 and 0–50% fly ash (FA) substitution for tidal exposure. They found that the ingress depth of 0.4% chloride by mass of binder was 18–21 mm already after 28 days, but only increased to 28–31 mm after ten years for concrete with 30% FA substitution [17]. Thomas and Matthews [17] plotted the ingress depth of 0.4% chloride by mass of binder versus the square root of time, but did not mention a linear relationship, although the graph indicated it.

Baroghel-Bouny et al. [18] found a linear relationship with a R^2 of > 0.95 between the average free chloride penetration depth measured by 0.1 N $AgNO_3$ spray test (assumed equal to 0.15% chloride by mass of binder) and the square root of the number of wetting–drying cycles after 10 years at marine tidal field exposure.

Based on the observations by Thomas and Matthews [17], Baroghel-Bouny et al. [18], Poulsen and Sørensen [15] and Poulsen et al. [16] it is likely that the observation of an ingress depth versus square root of time dependency can be generalized. The square root observation is based on a very simple linear relationship between the ingress depth of a single reference

concentration and the square root of exposure time. This linear relationship is consistent with the error function solution to Fick's 2nd law of diffusion for a semi-infinite medium with constant D_a and C_s [5]. However, the square root observation adds an intercept value to account for early ingress.

This paper formulates the square root observation as a method and analyzes the applicability to describe chloride ingress by including field data from submerged, tidal, atmospheric and inland deicing salt exposure at various geographical locations. Five different reference concentrations were analyzed for each exposure condition and geographical location. By applying the square root method on additional exposure conditions, it can be tested under which conditions the square root method is applicable.

2 Data

This paper analyzes data from a number of studies of in-situ exposed concretes from marine field exposure sites including exposure sites at Fehmarn, Denmark [16]; Träslövsläge, Sweden [19]; Østmarksneset, Norway [20] and Dornoch, Scotland [21]. Analyzed marine exposure conditions include submerged, tidal, splash and atmospheric. Further analyzed are data from concretes exposed in deicing environment at the inland field exposure site RV40, Sweden [22]. For each concrete composition and exposure condition data from three to eight exposure times, ranging from six months and up to maximum 31 years, were reported.

An overview of exposure conditions, curing and sampling is given in Table 1. An overview of mixture proportions of the analyzed concretes is given in Table 2. All cement notations are according to EN 197-1 [23]. The nomenclature (IDs) used in this study reflects the exposure site and the original ID used in the reference paper. When results obtained from the concretes are displayed in figures, the label additionally includes the content of supplementary cementitious materials (SCMs) and information on the exposure type, e.g. F-G12FA4SF_sub stands for Fehmarn Belt Exposure Site, concrete G, which include 12% fly ash (FA) and 4% silica fume (SF) and is exposed at submerged exposure. Binder types are described in groups comprising plain Portland cement (PC) and blends with FA, SF, ground granulated blast furnace slag (GGBS) and combinations of fly ash and silica fume (FA + SF).

3 The square root method for chloride ingress prediction

The square root dependency of a constant (reference) chloride concentration, C_r, proposed for chloride ingress prediction by Poulsen and Sørensen, was used to analyze the data [15, 32]:

$$x_{C_r}(t) = a_{C_r} \times \sqrt{t} + b_{C_r} \quad (2)$$

where t is the exposure time, $x_{Cr}(t)$ is the depth of C_r at t, and a_{Cr} and b_{Cr} are constants.

The method was applied using the steps described in Fig. 1.

3.1 Selection of input data for the square root method

In this study, only data sets with minimum three exposure times were used, and for which the chloride fronts penetrating from opposing sides of the specimens did not overlap. The entire data set (data from all exposure times) was omitted when lower chloride ingress was measured at a given exposure time relative to an earlier exposure time. This was the case for the combinations of concrete and exposure listed in Table 3.

A minimum exposure time of 200 days was applied in this study and the applicability of the data from the first exposure time was checked (see Sect. 5.1). The minimum exposure time was selected based on studies by Tang [33]. Investigating a range of binders (PC, SF) and w/b (0.32–0.70) Tang [27] found six months as sufficient time for laboratory samples to obtain an insignificant change of properties [e.g. water assessable porosity and diffusivity determined by the rapid chloride migration test (RCMT)] for prediction of free and total chloride ingress in submerged marine concrete using the so-called engineering expression of the ClinConc model [1].

3.2 Selection of input parameters for the square root method

Based on the range of observed $C_{max\text{-}t1}$ values (see Online Resource 1), two sets of C_r values were chosen.

Table 1 Overview of exposure conditions, curing and sampling at included exposure sites

Exposure	Marine				Deicing
Exposure site	Fehmarn	Träslövs läge	Østmarks neset	Dornoch	RV40
Main reference(s)	[16]	[19]	[20]	[21]	[22, 24, 25]
Number of concrete types	14	11	3 (6[a])	1	1
Exposure					
Marine					
Submerged	×	×		×[b)]	
Tidal	×		×	×	
Splash				×	
Atmospheric		×		×	
Inland					
Deicing					×
Avg. temperature (atmosphere) (°C)	10[c]	8[d]	5[e]	9[f]	6[f]
Avg. temperature (seawater) (°C)	9 [g]	11 [h]	8[e]	9[i]	NA
Chloride content (seawater) (g/l)	7 [g]	14 [h]	17[e]	20[i]	NA
Age at exposure					
(days)	–	9–19	28[e]	35[i]	37[j]
(maturity days)	40–49	–	28[e]	–	–
Thickness of specimens (mm)	200	100	500	1593	300
Sampling (years)	0.5, 2, 5	0.7, 1, 2, 5, 10, 20	1.5, 14, 21.5, 31	1.3, 2.3, 2.8, 3.3, 4.2, 5.5, 6.3, 21	1–2, 5, 10, 20
Diameter of extracted cores (mm)	100	100	100	30	100
Method for chloride analysis	[k]	[k]	[l] (1.5 years) [m] (14 years +)	[n]	[k]
Method for paste correction	[o]	[o]	[p]	[q]	[o]

[a]Pairwise identical

[b]Concrete exposed below mid tide level claimed to be permanently saturated, although not permanently submerged[21]

[c][26]

[d][27]

[e][20]

[f][28]

[g][29]

[h][19]

[i][30]

[j][22, 31]

[k]Profile grinding followed by potentiometric titration principally in accordance with AASHTO T260/NT BUILD 208

[l]Sawing of discs. Crushed and boiled in distilled water followed by potential measurements

[m]Profile grinding followed by nitric acid treatment and spectrophotometric analyses with iron thiocyanate as color indicator in accordance with SINTEFs procedure KS70 109

[n]BS1881 part 124 and BS 6337 part 4

[o]Chloride content corrected for potential variations in paste content as function of profile depth by using measured calcium profiles

[p]Calculated based on concrete composition

[q]Unknown

Table 2 Mixture proportions of concretes used in this study

Field exposure site	Fehmarn													
Concrete ID in this study	F-A	F-B	F-C	F-D	F-E	F-F	F-G	F-H	F-I	F-J	F-K	F-L	F-M	F-N
Mixture proportions of concrete exposed at Fehmarn Belt Exposure Site (kg/m^3) [16]														
Original concrete ID	A	B	C	D	E	F	G	H	I	J	K	L	M	N
Powder composition (wt%)														
CEM I	100	85	75	75	96	84	84	84	84	84				
FA[a]		15	25	25		12	12	12	12	12				
SF[b]					4	4	4	4	4	4				
CEM III											100	100	100	100
CEM I-SR5 42.5 N[c]	365	322	300	336	340	300	310	276	330	350				
CEM I 52.5 N[c]														108
CEM III/B 42.5 N[c,d]											360	375	410	
FA		57	100	112		43	44	39	47	50				
SF (added as slurry)					14	14	15	13	16	17				
GGBS[e]														252
Water	146	140	140	157	147	140	145	145	135	163	144	150	164	144
Sand	695	671	642	678	695	677	731	700	671	687	689	702	686	689
Coarse aggregates	1172	1182	1179	1053	1172	1192	1182	1182	1182	1067	1161	1185	1065	1162
w/(c + 2SF + 0.5 FA)	0.40	0.40	0.40	0.40	0.40	0.40	0.40	0.45	0.35	0.40	0.40	0.40	0.40	0.40
w/b[f]	0.40	0.37	0.35	0.35	0.42	0.39	0.39	0.44	0.34	0.39	0.40	0.40	0.40	0.40

Field exposure site	Träslövsläge										
Concrete ID in this study	T-1	T-OE	T-2	T-3	T-10	T-12	T-H1	T-H2	T-H4	T-H5	T-H8
Mixture proportions of concrete exposed at Träslövsläge Field Exposure Site (kg/m^3) [19]											
Original concrete ID	1–35	OE	2–40	3–35	10–40	12–35	H1	H2	H4	H5	H8
Powder composition (wt%)											
CEM I	100	100	100	95	78.5	85	95	90	95	95	80
FA					17	10					20
SF				5	4.5	5	5	10	5	5	
CEM I-SR5 42.5 N					330						
CEM I-SR3 42.5 N	450	430		428		383	475	450	399	523	493
CEM I 42.5 R			420								
FA					71	45					123
SF (added as slurry)							25	50	21	28	
SF (added as powder)				23	19	23					
Water	158	163	168	158	148	146	150	150	168	138	159
Sand	839	813	871	801	770	781	836	820	840	806	680
Coarse aggregates	839	840	804	868	905	917	942	963	840	946	865
w/(c + 2SF + 0.5 FA)	0.35	0.38	0.40	0.33	0.37	0.33	0.29	0.27	0.38	0.24	0.29
w/b	0.35	0.38	0.40	0.35	0.35	0.33	0.30	0.30	0.40	0.25	0.26

Field exposure site	Østmarkneset						Dornoch	RV40
Concrete ID in this study	Ø-EF	Ø-EF	Ø-GH	Ø-GH	Ø-IJ	Ø-IJ	Dor	RV206
Mixture proportions of concrete exposed at Østmarkneset [20], Dornoch [21] *and RV40 field exposure sites* (kg/m^3) [22, 24, 25]								
Original concrete ID	E	F	G	H	I	J		206

Table 2 continued

Field exposure site	Østmarkneset						Dornoch	RV40
Concrete ID in this study	Ø-EF	Ø-EF	Ø-GH	Ø-GH	Ø-IJ	Ø-IJ	Dor	RV206
Powder composition (wt%)								
CEM I	80	80	90	90	80	80	100	95
SF	20	20	10	10	20	20		5
CEM I 52.5 R	234	234	457	457	394	394		
CEM I 42.5 N							460	
CEM I-SR3 42.5 N								399
SF (as slurry)	47	47	46	46	79	79		21
Water	194	194	204	204	218	218	184	168
Sand	847	847	752	752	749	749	700	860
Coarse aggregates	1032	1032	919	919	905	905	1050	860
w/(c + 2SF + 0.5 FA)	0.59	0.59	0.37	0.37	0.40	0.40	0.40	0.38
w/b	0.69	0.69	0.41	0.41	0.46	0.46	0.40	0.40

[a]FA = Fly ash

[b]SF = Silica fume (dry matter)

[c]According to EN 197-1

[d]GGBS content: 67 wt%

[e]GGBS = Ground granulated blast furnace slag

[f]Water-to-binder ratio (by mass)

One set for submerged and tidal exposure and another set for splash, atmospheric, and deicing exposure, see Table 4. When choosing the maximum C_r value a compromise was made between (1) ensuring that all C_r values could be applied for all concretes (maximum $C_r \leq$ minimum $C_{max\text{-}t1}$) and (2) including the widest possible span of C_r values. The compromise was made slightly below the 20th percentile of the $C_{max\text{-}t1}$ values, thus ensuring that all C_r values were tested for at least 80% of the concretes. The remaining up to 20% of the concretes (see Table 4) were still tested at lower C_r values present in those concretes. Additionally, four reference concentrations were chosen as the pentiles. All chloride profiles are given in Online Resource 1 with the utilized C_r values marked as horizontal lines.

4 Results

Before applying the square root method on all the data (Sect. 2), it was checked, whether the assumption made in the methods section (Sect. 3), that a_{Cr} is constant, when using data after minimum 200 days exposure ($t1$), is correct.

4.1 Applicability of the chosen $t1$

Initially, it was verified whether the $t1$ applied in this study i.e. 203–370 days, is sufficient to have reached insignificant changes of properties as mentioned in Sect. 3.1. The result of this verification is seen at Fig. 2, where the ingress depth of $C_r = 0.75\%$ chloride by mass of binder ($x_{0.75}$) at t1 predicted by the square root method using data from $t2$ and $t3$ is compared to the ingress depth found by linear interpolation on the measured chloride profiles for $t1$. Data from submerged exposure for Fehmarn Belt and Träslövsläge Field Exposure Sites (Fig. 2a) as well as data from tidal exposure from Fehmarn Belt Exposure Site (Fig. 2b) was used for this comparison.

The data points are closely distributed around the line $x = y$ with a single outlier on either side, which indicate, that the chloride profiles from $t1$, can be used in the square root method without any systematic change of a_{Cr} and b_{Cr}. The remaining data series show similar behavior. This implies that for the investigated concretes and exposures, the quality of the datapoint ($x_{Cr\text{-}t1}$, $t1$) is as good as the remaining data points.

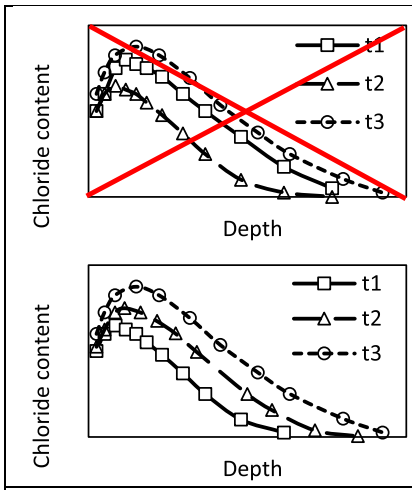

Step 1

Chloride ingress profiles for minimum three exposure times (t1, t2, t3) were collected.

It was checked that the chloride content increased with time (lower graph). If not, the entire data set (data from all exposure times) was omitted (upper graph).

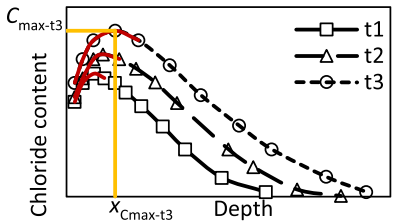

Step 2

For each chloride profile, the value ($C_{max\text{-}t}$) and depth ($x_{Cmax\text{-}t}$) of the maximum chloride content was identified (here shown for t3).

All data for $x \leq x_{Cmax-t}$ was discarded.

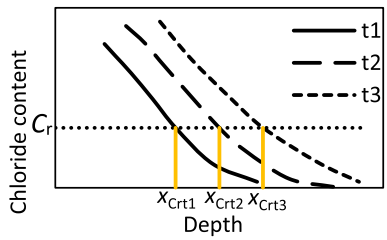

Step 3

A reference concentration (C_r), C_r<$C_{max\text{-}t1}$ was selected (dotted line).

For each chloride profile, the ingress depth (x_{Cr}) for chloride content (C) where C = C_r was identified. Linear regression between nearest measuring points of C_r was used.

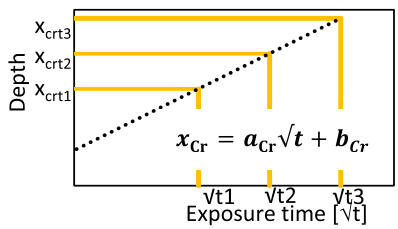

Step 4

x_{Cr} vs the square root of exposure time was plotted and the slope (a_{Cr}) and the intercept (b_{Cr}) determined by linear regression.

Fig. 1 Application of the square root method for determination of the chloride ingress constants a_{Cr} and b_{Cr} (Eq. 3)

4.2 Application of the square root method

Data from 59 combinations of exposure site, exposure condition and concrete were treated by the method described in Fig. 1 for five different C_r values. The resulting a_{Cr}, b_{Cr} and R^2 values (237 sets in total) are tabulated in Online Resource 2.

Figure 3 illustrates the results of the application of the square root method at five different C_r values on

Table 3 Excluded combinations of concrete and exposure conditions due to measured lower chloride ingress at a given exposure time relative to an earlier exposure time

Exposure	Fehmarn (see Table 2)	Träslövsläge (see Table 2)
Submerged	F-A, F-C	T-1, T-3
Tidal	F-F	–
Atmospheric	–	T-OE, T-H2, T-H3, T-H5, T-H8

Table 4 Range, average and 20th percentile of observed $C_{max\text{-}t1}$ and chosen range of C_r for all analyzed concretes and exposure types

Exposure	$C_{max\text{-}t1}$ (% by mass of binder)			Sets of selected C_r (%by mass of binder)	Concretes, where max C_r was not present at t1 (see Online Resource 1)
	Range	Average	20th percentile		
Submerged	0.68–3.62	2.01	1.38	0.25, 0.50, 0.75, 1.00 and 1.25	F-M, F-N, T-H5
Tidal	0.44–3.70	2.07	1.37		F-M
Splash	0.76–0.78	0.77	[a]	0.10, 0.20, 0.30, 0.40 and 0.50	
Atmospheric	0.65–0.93	0.83	0.73		
Deicing	0.80	0.80	[a]		

[a]Too little data to perform statistical analysis

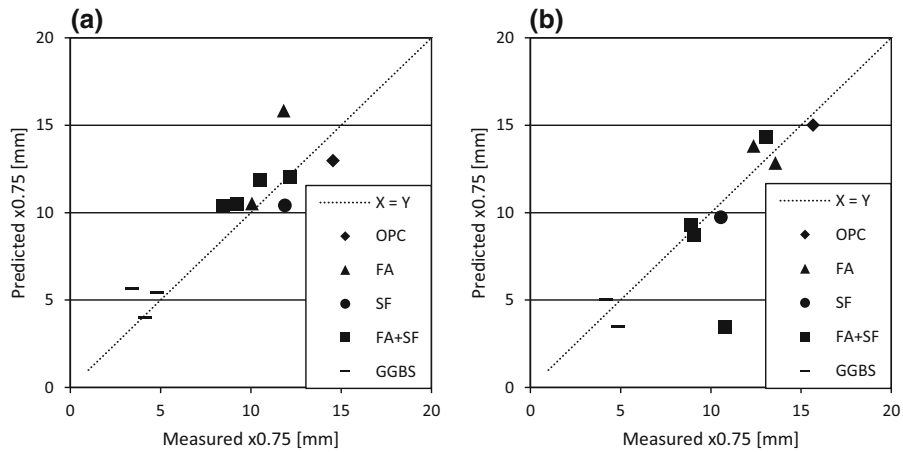

Fig. 2 The ingress depth of a concentration of 0.75% chloride by mass of binder ($x_{0.75}$) at $t1$ predicted by the square root method using data from $t2$ and $t3$ compared to the ingress depth found by linear interpolation on measured data for $t1$. $t1$ varied between 203 and 217 days. **a** Data from submerged exposure for Fehmarn and Träslövsläge was used. **b** Data from tidal exposure from Fehmarn was used. A dotted straight line corresponding to $x = y$ is drawn as guidance

concrete T-H8 submerged exposed at Träslövsläge Field Exposure Site.

5 Discussion

This section includes discussions on the impact of the choice of C_r on a_{Cr}, b_{Cr}, R^2 and x_{Cr}. Further the impact of exposure condition and binder is treated and hypotheses for the observed linearity of x_{Cr} versus

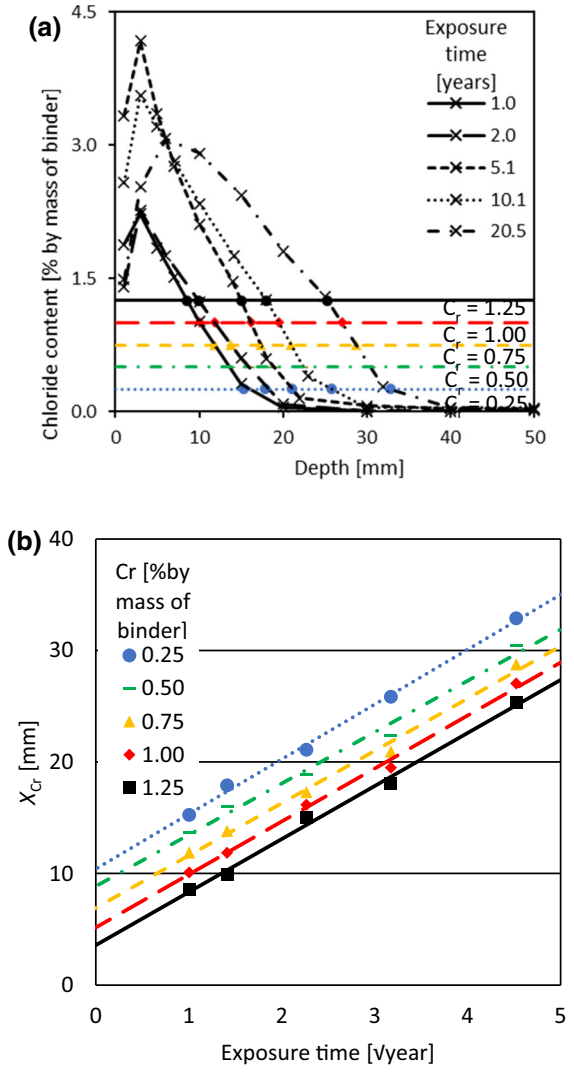

Fig. 3 Application of the square root method at five different C_r values (in % chloride by mass of binder) on concrete T-H8 submerged exposure at Träslövsläge Field Exposure Site. **a** Example of application of step 3 of the square root method (see Fig. 1). Concrete T-H8 exposed submerged at Träslövsläge Field Exposure Site (see Table 3). Interpolated ingress depths of C_r = 0.25, 0.50, 0.75, 1.00 and 1.25% chloride by mass of binder are marked with symbols. **b** Example of application of step 4 of the square root method (Eq. 3; see Fig. 1). Concrete T-H8 submerged exposed at Träslövsläge Field Exposure Site (see Table 3). x_{Cr} = penetration depth of C_r

$\sqrt{t}$ are proposed. Finally, the ability of the square root method to predict further ingress is evaluated and suggestions are given on how to use the method.

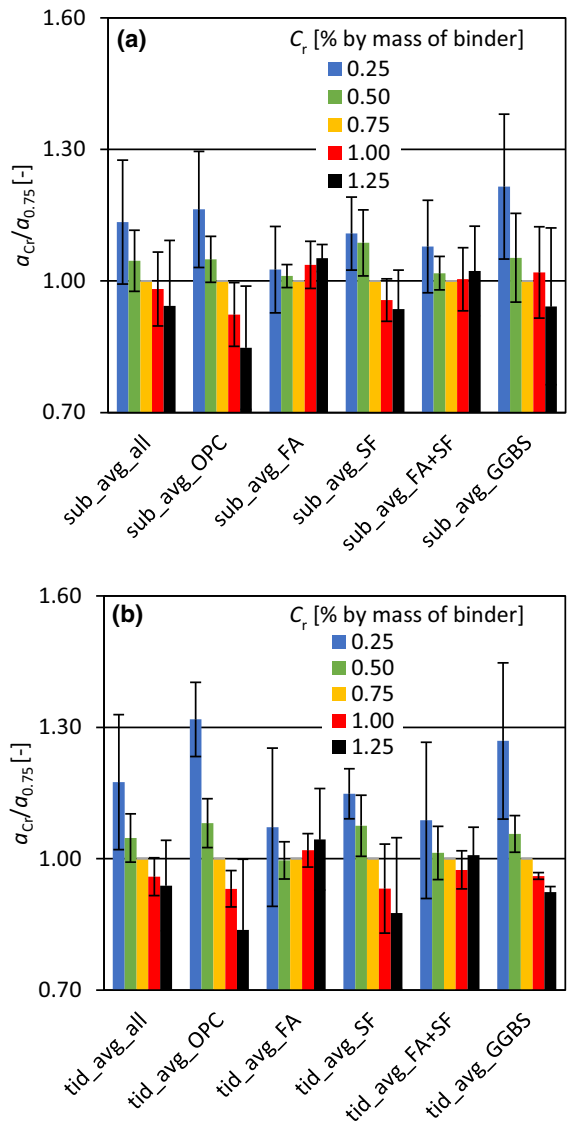

Fig. 4 Influence of chosen C_r on average a_{Cr} value for concretes based on different binders in **a** submerged and **b** tidal exposure. Note that a_{Cr} is normalized to $a_{0.75}$. Error bars show ± 1 standard deviation

5.1 Impact of reference concentration, C_r

As mentioned in Sect. 3, to apply the square root method a reference concentration, C_r, must be chosen. In this section, the influence of the chosen C_r is discussed. The datasets for submerged and tidal exposure are used, as they represent the widest variety of concretes and identical C_r values, see Online Resource 2.

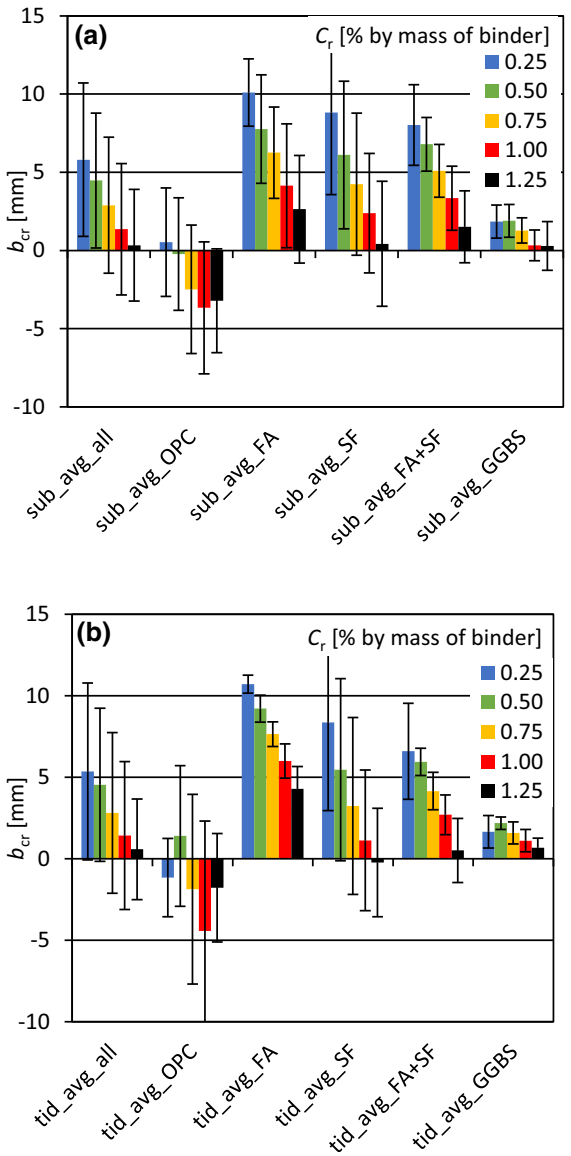

Fig. 5 Influence of chosen C_r on average b_{Cr} value for concretes based on different binders in **a** submerged and **b** tidal exposure. Error bars show ± 1 standard deviation. Note that the values of b_{Cr} are not normalized as some $b_{0.75}$ are near zero and the corresponding concretes thus affect the average too much

The influence of C_r on a_{Cr}, b_{Cr} and R^2 is separated by binder type and exposure to highlight potential differences. The influence of binder is further treated in Sect. 5.4.

5.1.1 Impact of C_r on a_{Cr}

Figure 4 shows the calculated ingress parameter, a_{Cr}, as a function of the reference chloride concentration, C_r, for submerged conditions (Fig. 4a) and tidal conditions (Fig. 4b). For each combination of concrete and exposure, a_{Cr} is normalized to $a_{0.75}$. Thereafter the results are grouped and averaged per binder type (PC, FA, SF, FA + SF, GGBS); see Online Resource 3 for an example of how data is normalized and averaged. From Fig. 4 it is seen, that there is in general a slightly decreasing trend of $a_{Cr}/a_{0.75}$ with increasing C_r. This trend is most pronounced for PC, SF and GGBS containing concretes, whereas $a_{Cr}/a_{0.75}$ for concretes with FA (FA and FA + SF) is almost independent of the C_r. The varying dependency between binders of $a_{Cr}/a_{0.75}$ on C_r implies that $a_{Cr}/a_{0.75}$ could be higher for a concrete based on binder i than binder ii at one C_r, while the opposite is the case at another C_r (See Online Resource 4).

Figure 4 shows decreasing $a_{Cr}/a_{0.75}$ with increasing C_r. This means, that the calculated ingress parameter is lower for higher C_r. Physically this observed trend coincide with a reduction in the driving force for diffusion, as the concentration gradient decreases with increasing C_r (all other things being equal).

When comparing the results from submerged exposure (Fig. 4a) with the ones from tidal exposure (Fig. 4b), there is a trend that $a_{0.25}/a_{0.75}$ is higher for tidal exposure than for submerged exposure irrespective of the binder type.

5.1.2 Impact of C_r on b_{Cr}

The impact of the selected C_r on b_{Cr} is illustrated in Fig. 5. It is seen that b_{Cr} depends on both C_r and the binder composition. A clear decreasing trend of b_{Cr} with increasing C_r is seen for FA, SF and SF + FA containing concretes independent of exposure condition (submerged and tidal). The analyzed PC and GGBS containing concretes have b_{Cr} values near 0 irrespective of C_r in the range 0.25–1.25. This implies that a_{Cr} governs the chloride ingress for the analyzed PC and GGBS concretes.

Figure 5 shows a decreasing b_{Cr} with increasing C_r. This might be explained by two competing sets of mechanisms:

(i) Capillary suction and high diffusivity at early age

Poulsen et al. [16] interpreted b_{Cr} as partly due to initial capillary suction due to self-desiccation or partial drying and partly due to limited degree of hydration resulting in a concrete, which is initially more permeable than in a more mature state. Thus, it is expected that chloride ingress proceeds faster initially, than what can be described by a_{Cr} alone. This leads to a positive contribution to b_{Cr}.

(ii) Gradual phase changes and increasing C_{max}.

Selecting a high C_r which is only present in the concrete after e.g. 4 years, the intercept at the x-axis of the straight line constituting x_{Cr} versus the square root of time (step 4, Fig. 1) would be 2 ($\sqrt{4}$). As the ingress parameter a_{Cr} is positive, this implies that b_{Cr} is negative. An increasing C_{max} could e.g. be caused by phase changes as ions from the sea water such as chloride are bound in the system and others leached [13, 34]. The higher the chosen C_r, the longer time it will take for the reference concentration to be present in the concrete and the larger the negative contribution on b_{Cr} will be.

The set of mechanisms (1) is relatively independent of C_r and therefore relatively more pronounced at low C_r, whereas the set of mechanisms (2) is concentration dependent and more pronounced at high C_r. As b_{Cr} is the sum of positive and negative contributions, the result is a decreasing b_{Cr} with increasing C_r.

5.1.3 *Discussion on limits of reference concentration*

For service life modeling the reference concentration of interest is typically the critical chloride content causing corrosion initiation. However, the critical chloride content can vary considerably [35, 36]. It is therefore important to know the range of reference concentrations with which the square root method can be applied.

Choosing a C_r value higher than the maximum chloride content at the earliest recorded exposure times naturally rules out the use of these chloride profiles for the square root method. Additionally, for a fixed exposure time, it forces the use of a point closer to the concrete surface, which could potentially lead to disturbances caused by leaching and elemental zonation [13, 34].

The lower limit of the C_r value must be related to the method of obtaining the chloride profile, as well as the detection limit and accuracy. The lowest C_r value

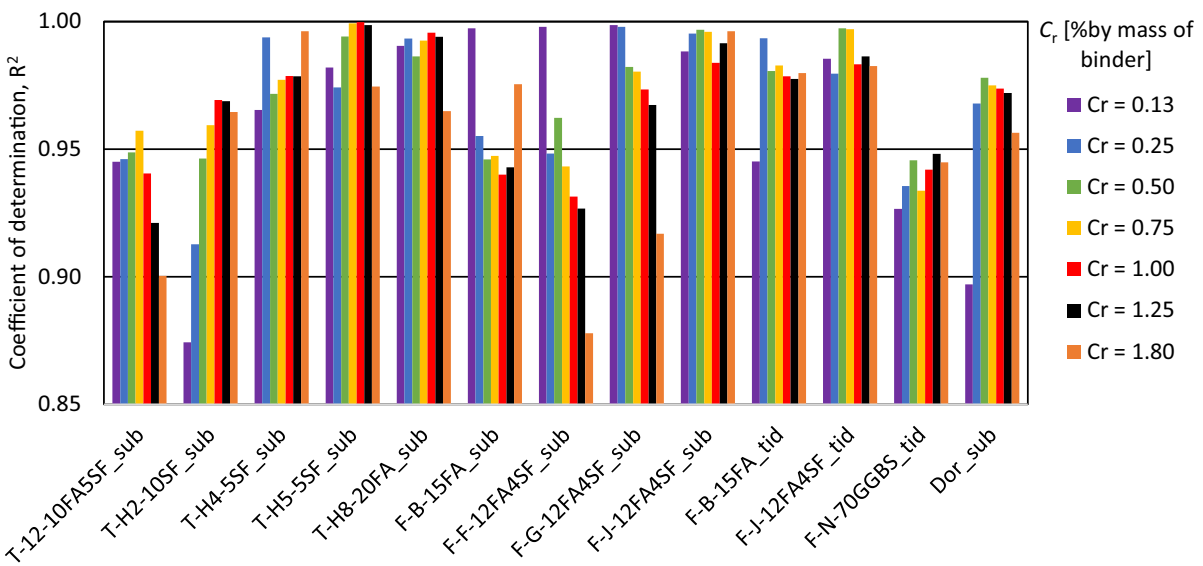

Fig. 6 R^2 value of linear regression on x_{Cr} versus square root of time for five concretes from submerged exposure at Träslövsläge Field Exposure Site, when using C_r values of 0.125 and 1.8% chloride by mass of binder in comparison to the five C_r values used throughout this study for submerged and tidal exposure

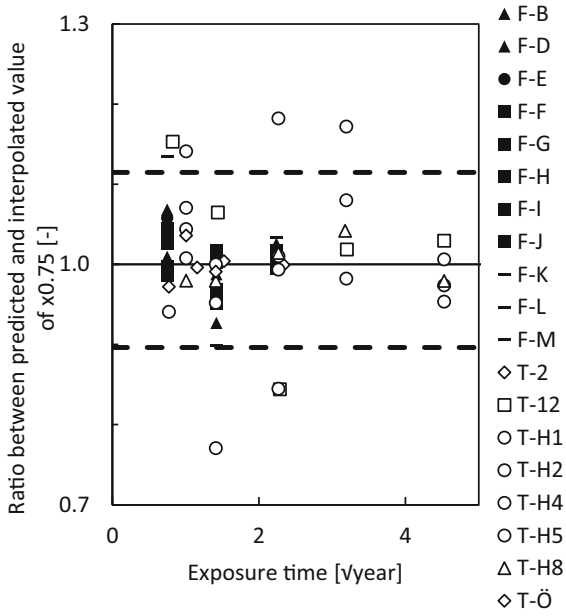

Fig. 7 Ratio between $x_{0.75}$ predicted by Eq. (1) ($x_{Cr}(t) = a_{Cr}\sqrt{t} + b_{Cr}$) and measured by linear interpolation between the nearest data points directly below and above the reference concentration (0.75% chloride by mass of concrete). white fill = Fehmarn, black fill = Träslövsläge, diamond = PC, triangle = FA, circle = SF, square = FA + SF, line = GGBS. The dashed lines show a 90% confidence interval

must be distinguishable from the initial chloride content (C_i). Further, to enable interpolation, the profile grinding must be conducted deep enough to detect a concentration lower than the lowest C_r value.

To test the chloride concentration range in which the method is applicable; the square root method was applied on concretes exposed in submerged and tidal zones for C_r values of 0.125 and 1.8% chloride by mass of binder. (Note that for some of the combinations, the highest concentration was not reached at the shortest analyzed exposure time.) From Fig. 6 it can be seen that R^2 for both C_r values was comparable to R^2 for the C_r values generally used in this paper (see Table 4), except when using C_r = 1.8% chloride by mass of binder for T-12, F-F and F-G and C_r = 0.125% chloride by mass of binder for T-H2 and Dor_sub, where a decreasing tendency of R^2 is observed. It can be concluded that the square root method is valid for the investigated concretes in submerged and tidal exposure for the whole range of tested C_r values, i.e. 0.125–1.80% chloride by mass of binder. Similarly, the method was found applicable for concretes in the atmospheric zone using C_r values in the range 0.1–0.5% chloride by mass of binder (data not shown here).

5.1.4 *Selection of C_r for remaining discussion*

When investigating the influence of exposure conditions and binders in further detail, it was chosen to proceed with a C_r of 0.75% chloride by mass of binder for tidal and submerged exposure. For atmospheric and deicing exposure, it was chosen to proceed with a C_r of 0.3% chloride by mass of binder. These reference concentrations were chosen from a perspective of benefitting from using as much of the raw data as possible, i.e. avoiding the challenge of using a C_r which is yet not obtained at t1 or which is not measured due to lack of grinding depth. In theory, if the chloride threshold value is known and within the limits of reference concentrations discussed in Sect. 5.1.3, it could be chosen as C_r.

5.2 Accuracy of interpolation

Figure 7 shows the ratio between the ingress depth of C_r = 0.75% chloride by mass of binder calculated by the square root method by using data from all available exposure times, and the ingress depth found by linear interpolation between the nearest data points directly below and above the C_r in the measured chloride profiles ($x_{0.75}$(predicted)/$x_{0.75}$(measured)).

For the analyzed concretes, $x_{0.75}$(predicted)/$x_{0.75}$(measured) varied by ± 11% (90% confidence interval). The largest variation is observed for concretes containing SF, whereas the least variation is observed for concretes with PC or FA. Considering the usual variation in service life estimates, a prediction error of 11% (90% confidence interval) appears acceptable [21, 37, 38].

5.3 Impact of exposure condition

Considering a_{Cr} describes the ingress of chloride ions over the square root of time, a given concrete should have a higher a_{Cr} value, the higher the environmental load it is exposed to. The environmental load can be described by chloride, moisture and temperature load. When tidal, submerged and atmospheric exposure are compared, a_{Cr} is expected to be lowest for atmospheric exposure due to the relatively low chloride and

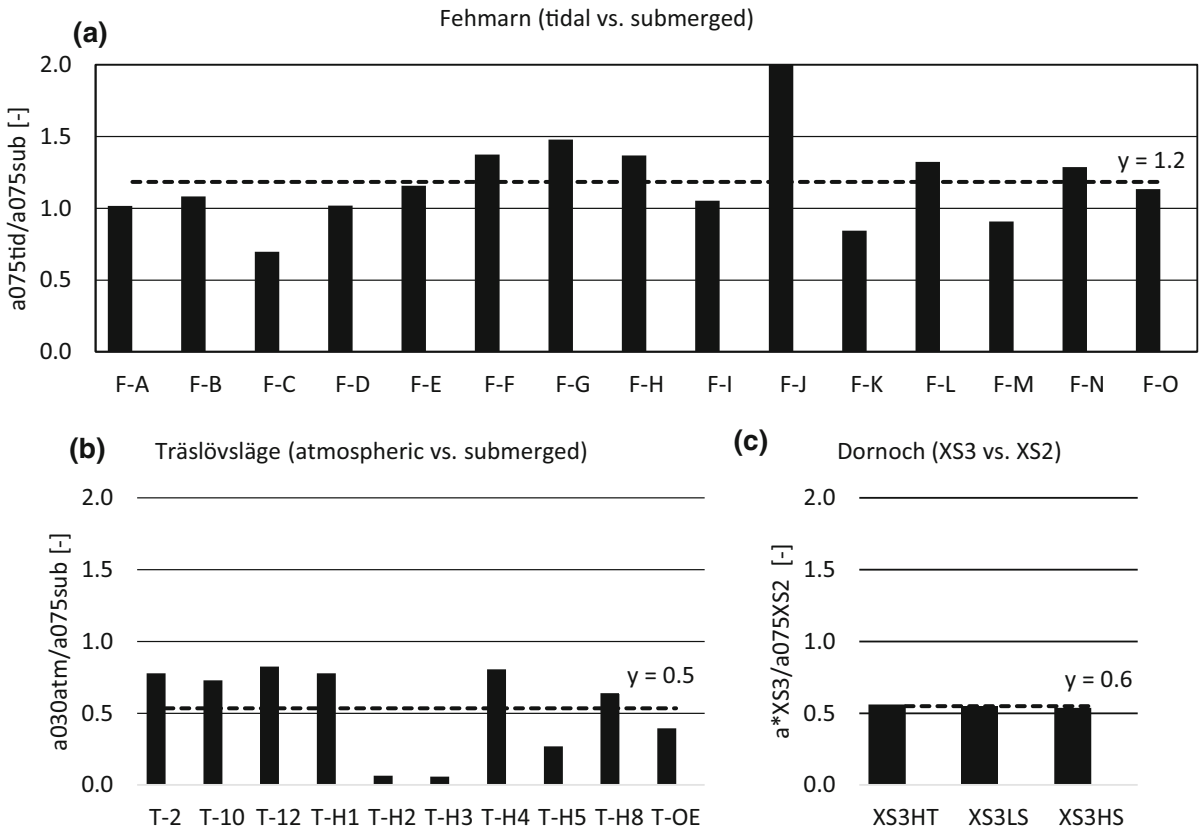

Fig. 8 **a** Ratio between $a_{0.75}$ for concretes in tidal vs. submerged exposure at Fehmarn Belt Exposure Site. The dashed line indicates the average ratio. **b** Ratio between $a_{0.30}$ for concretes in atmospheric versus $a_{0.75}$ for concretes in submerged exposure at Träslövsläge Field Exposure Site. The dashed line indicates the average ratio. **c** Ratio between a_{Cr} for the concrete Dor exposed at XS3HT (high tide, $C_r = 0.75$), XS3LS (low splash, $C_r = 0.75$) and XS3HS (high splash, $C_r = 0.30$) versus XS2 (below mid tide, $C_r = 0.75$) at Dornoch Field Exposure Site. The dashed line indicates the average ratio

moisture load present there. The relative ingress rate in the tidal and submerged exposure is expected to be depth dependent; in the tidal zone convection will cause rapid ingress and accumulation of chlorides in the surface near region giving rise to a high chloride gradient, whereas an expected higher moisture state of submerged concrete will facilitate a higher diffusion coefficient [39].

As shown in Table 1, in this study data has been analyzed from three exposure sites, where elements of the same concrete composition are exposed under different exposure conditions. A comparison between a_{Cr} at $C_r = 0.75$ (submerged, tidal, low splash) and $C_r = 0.3$ (atmospheric, high splash) for identical concretes in different exposure conditions is shown in Fig. 8a–c.

For Dornoch Field Exposure Site no data is available for submerged exposure. However, one concrete composition is exposed in almost saturated below mid tide level and thus used as reference [21].

Figure 8a–c indicates that for the compared exposure conditions, a_{Cr} depends not only on the material, but also on the exposure. Large variations are observed between concrete compositions. However, for the investigated combination of concretes, exposure conditions and C_r, a_{Cr} typically descended in the order: tidal > submerged > atmospheric, high tidal and splash. The mentioned order of descension did not change by varying C_r within the investigated span (not reported here). Note that lower C_r values were used for atmospheric and high splash exposure than for submerged. However, due to the increasing trend of a_{Cr} with decreasing C_r (Fig. 4), the ratio is expected to be lower, if a_{Cr} for atmospheric and splash exposure was compared to a_{Cr} for submerged exposure at the same C_r. Thus, this effect would increase the influence

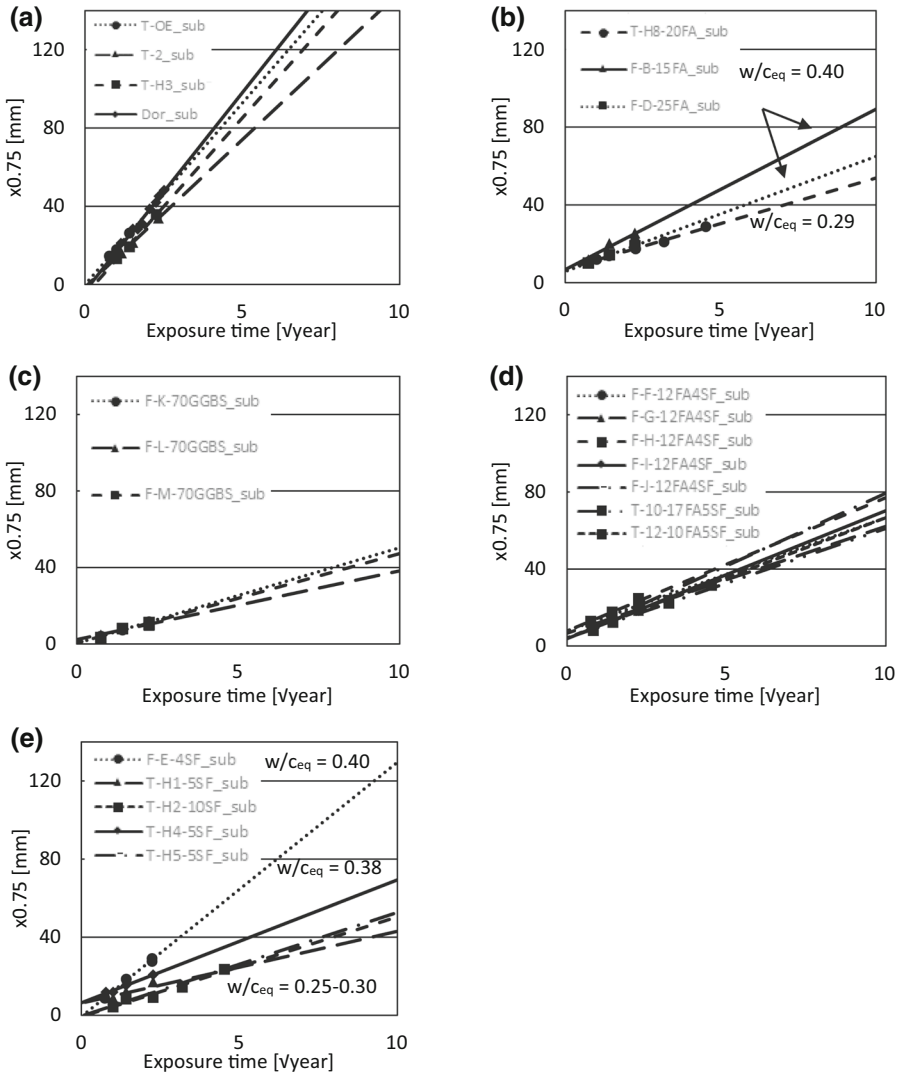

Fig. 9 Experimental data (markers) and graphical result of the square root method (lines) for concretes in submerged exposure. **a** PC, **b** FA, **c** GGBS, **d** FA + SF, **e** SF. C_r = 0.75. Although concretes with similar binders are compared for submerged exposure and identical C_r, some differences are seen between the concretes due to differences in w/c_{eq}, exposure temperature, salinity etc

of environment as compared to what is shown in Fig. 8a–c.

The square root method was applied on data for deicing exposure from the highway RV40 field exposure site in Sweden [22, 24, 25]. However, only a single concrete complied to the criteria set up in Sect. 3.1. The other concrete compositions failed on the criterium of having an increasing chloride concentration with time. This could partly be due to seasonal changes as de-icing salts are spread during the cold seasons and the chloride profiles were measured at different times of the year (January, May, June, July and September). Further the de-icing procedure changed, while the data collection was ongoing. When only summer sampling (May–July) from vertical surfaces is utilized for concrete 206, R^2 values of 0.98–1.0 are obtained—see Online Resource 2. However, as data from only a single concrete in de-icing exposure complied to the criteria set up in Sect. 3.1 and the data due to seasonal variations is expected less reliable, de-icing is not treated further.

5.4 Influence of binder

Based on the findings in Sects. 5.1 and 5.3, the analysis on the influence of binders is conducted for a fixed C_r of 0.75 and submerged exposure conditions. Submerged exposure is chosen as the widest variety of binder compositions is available for this exposure condition. Figure 9 shows the experimental and

Table 5 a_{Cr}, b_{Cr} and R^2 values for concretes in submerged exposure. Binder groups are divided by thick borders (FA = Fly ash, GGBS = Ground granulated blast furnace slag, SF = Silica fume). C_r = 0.75

Binder	Concrete	a_{Cr} (mm/$\sqrt{}$year)	b_{Cr} (mm)	R^2 (−)	Predicted ingress after 100 years (mm)	Binder	Concrete	a_{Cr} (mm/$\sqrt{}$year)	b_{Cr} (mm)	R^2 (−)	Predicted ingress after 100 years (mm)
PC	T-OE	18.6	0	0.99	186	FA	T-H8	4.7	7	0.99	54
	T-2	15.1	− 1	1.00	150		F-B	8.3	7	0.95	90
	T-H3	18.1	− 6	1.00	175		F-D	5.9	6	1.00	65
	Dor	20.3	− 3	0.97	200	GGBS	F-K	5.0	0	1.00	50
FA + SF	F-F	5.9	8	0.94	67		F-L	3.6	2	0.96	38
	F-G	5.6	7	0.98	63		F-M	4.7	0	0.94	47
	F-H	6.9	8	0.95	77	SF	F-E	13.0	− 1	0.99	129
	F-I	6.6	4	0.99	70		T-H1	3.7	6	0.87	43
	F-J	7.6	4	1.00	80		T-H2	5.1	− 1	0.96	50
	T-10	5.7	4	1.00	61		T-H4	6.3	6	0.98	69
	T-12	6.2	4	0.96	66		T-H5	5.3	0	1.00	53

modelled chloride ingress data for concretes with different binder types (PC, FA, GGBFS, FA + SF and SF). Table 5 presents the corresponding parameters of the square root fits.

Note that the choice of C_r has an impact on the predicted chloride ingress as described in Sect. 4.2 i.e. if a lower C_r was chosen, the predicted chloride ingress in a PC concrete would be even higher relative to a FA containing concrete. An example of the influence of C_r on the ingress depth is given in Online Resource 4, where the graphical result of the square root method applied on concretes exposed at submerged exposure for C_r = 0.75 (as shown at Fig. 9) is compared to the graphical result for C_r = 0.25.

As expected, some differences are seen between the concretes in Fig. 9. Although concretes with similar binders are compared for submerged exposure and identical C_r, differences exist in w/c, exposure temperature, salinity etc. (see Table 1). a_{Cr} is e.g. expected to increase with increasing w/c.

From Fig. 9, Table 5, Online Resource 2 and Online Resource 3 it is seen that the regression coefficients are very high. Further it is noted that similarities exist between similar compositions. e.g. a_{Cr} of the analyzed PC concretes are all in the range 15–20 mm/$\sqrt{}$year, which is higher than for any other concretes. Contrary, b_{Cr} is low for the PC concretes. A low b_{Cr} combined with a high a_{Cr} is interpreted as the PC concretes quickly obtain their maximal potential chloride resistance in the given environment they are exposed to, but that this maximal potential chloride resistance is relatively poor (assuming similar moisture level).

The values of a_{Cr} obtained for FA, FA + SF and GGBS concretes are low compared to the PC concretes and they are all in the same range (4–8 mm/$\sqrt{}$year). The long-term chloride resistance is high for both FA, FA + SF and GGBS, but due to an additional high early resistance, reflected in the low b_{Cr}, the GGBS concretes have the lowest extrapolated ingress depths after 100 years as shown in Fig. 9c.

5.5 Hypotheses for linearity of x_{Cr} versus $\sqrt{t}$

The ingress of ions (1) in concrete might be explained by the Nernst–Planck equation (Eq. 1). The left hand term of the equation describes the change of concentration over time. The three right hand terms describe diffusion, migration and convection respectively [40]:

$$\frac{\partial c_i}{\partial t} = \nabla\left(D_i \nabla c_i + z_i u_{m,i} F c_i \nabla V - c_i v\right) \quad (1)$$

where c_i = ionic concentration, D_i = ionic diffusion coefficient, z_i = electrical charge, $u_{m,I}$ = the ionic mobility, F = Faradays constant, V = electrostatic potential, v = velocity of the solvent.

Assuming one-dimensional diffusion in a non-reactive and homogeneous media, the diffusion

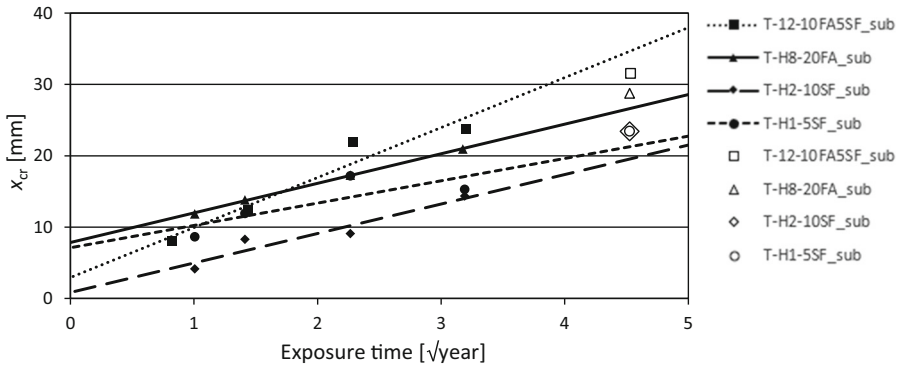

Fig. 10 Predicted versus measured chloride ingress (C_r = 0.75) at 20 years for four submerged concretes exposed at Träslövsläge Field Exposure Site. Prediction was made from data up to 10 years exposure (shown with filled markers). The diameter of the measured data point for T-H2-10SF_sub is doubled to distinguish it from that of T-H1-5SF_sub

coefficient is constant, and the diffusion is square root of time dependent.

At initial exposure to chloride ions, concrete is in general neither fully saturated nor fully hydrated. Therefore, initial ingress might be enhanced by capillary suction (convection) and a higher initial diffusion due to an initial higher and more interconnected porosity. The latter is especially expected for concretes containing slowly reacting SCMs as e.g. fly ash.

Over time it is expected that convection ceases or becomes insignificant compared to diffusion. However, other factors such as elemental zonation [13], leaching [41], moisture [42] and temperature [43] are also known to influence the ingress, binding and resulting chloride profiles. Predicting the ingress depth of a total fixed (reference) chloride concentration, the concentration dependency of chloride binding (illustrated with a non-linear binding isotherm), can be neglected. In addition, the potential impact of leaching and elemental zonation on chloride binding is reduced. Finally, focusing on deeper ingress depths, limited impact of moisture changes on the transport coefficient is expected.

In summary, when the dominant chloride ingress mechanism is diffusion and the diffusion coefficient and chloride binding capacity are constant, linearity is expected of x_{Cr} versus $\sqrt{t}$, as the square root of the diffusion coefficient is length/$\sqrt{t}$.

5.6 Ability to predict further ingress

To test the ability of the square root method to predict further ingress, the dataset from Träslövsläge Exposure Site comprising data from five exposure times up to 20 years was used. The square root method was applied to the first four data points (up to 10 years or 3.3 $\sqrt{}$year) and the predicted ingress after 20 years was compared to the measured ingress. The deviation between the predicted and measured ingress depth was similar for the measured ingress depths of $t1-t4$ to which the prediction was fitted (9% deviation) as to the measured ingress depth at $t5$, which was not used for fitting the straight line (12% deviation)—see Fig. 10 and Online Resource 5. It can therefore be concluded that the square root method is able to predict chloride ingress with an acceptable accuracy over 20 years.

5.7 Suggestions of how to use the square root method

The square root method is suggested to be used for (1) estimating remaining service life of existing structures. Depending on the availability of data, it might also be used for service life design of new structures.

When used for estimating the remaining service life of existing structures, the following information is required:

- Chloride threshold value. The reference chloride concentrations, C_r, should reflect the expected range of chloride threshold values for corrosion initiation.
- Cover depth.

- Chloride profiles to establish a straight line by the square root method considering the following aspects:
- Chloride profiles must be measured with a sufficient period in time between them to allow the difference in chloride content to exceed the measurement uncertainties.
- The exposure time of the first data point must be sufficiently long, so potential initial effects of e.g. capillary suction and prolonged hydration have ceased. The present investigation indicates the applicability of data from the earliest recorded exposure times (200 days for concrete initially cured for 43–49 maturity days and 217–370 days for concrete initially cured for 12–19 maturity days).
- Although two exposure times are sufficient to establish a straight line by the square root method, it is suggested to determine three profiles at minimum three exposure times. If any of the points deviate from the long-term trend (e.g. with R^2 less than 0.95), additional data points should be obtained.

When estimating the ingress depth for a long design service life (e.g. 100 years) by the square root method, the impact of a_{Cr} heavily exceeds that of b_{Cr} (see Table 5). Based on the findings in Sects. 5.1–5.4 multiple parameters including binder composition and exposure conditions do have an influence on the parameters a_{Cr} and b_{Cr}. There exists a potential of improving design values for new structures by increasing the number of investigated datasets and parameters to include e.g.:

- The influence of binder compositions.
- The influence of production and execution.
- The influence of exposure time and conditions.
- The influence of maintenance.

6 Conclusion

Based on analysis by the square root method of 34 concretes containing various amounts of PC, FA, SF and GGBS field exposed in up to five environments, it is concluded that:

- The ingress depth (x_{Cr}) of a fixed (reference) chloride concentration (C_r) in the investigated concretes followed a square root of time dependency: $x_{Cr}(t) = a_{Cr}x\sqrt{t} + b_{Cr}$, where a_{Cr} and b_{Cr} are constants.
- The square root method appeared valid for marine exposed concrete in submerged, tidal, splash and atmospheric zone. Too little data was available for assessing the applicability for concrete in de-icing exposure.
- The square root method was found to be valid for the whole range of tested C_r values (0.125–1.80% chloride by mass of binder for submerged, tidal and low splash; 0.1–0.5% chloride by mass of binder for high splash and atmospheric exposure).
- The square root method appeared valid for the investigated PC, SF, FA, FA + SF and GGBS containing concrete.
- For the analyzed concretes, $x_{0.75}$(predicted)/$x_{0.75}$-(measured) varied by ± 11% (90% confidence interval).
- For the investigated concretes and conditions, a_{Cr} was found to be constant after 200 days of exposure.
- A decreasing trend of a_{Cr} with increasing C_r was observed for submerged and tidal exposure. It was most pronounced for PC, SF and GGBS containing concretes.
- A clear decreasing trend of b_{Cr} with increasing C_r was observed for FA, SF and SF + FA containing concretes in submerged and tidal exposure.
- Based on a dataset from 1 to 10 years of exposure we were able to predict the chloride ingress after 20 years with a deviation of 12%.

In summary, the square root method seems to offer a reliable possibility to predict chloride ingress.

Acknowledgements The authors would like to thank Femern A/S, S. V. Nanukuttan and O. Skjølsvold for sharing field data from the field exposure sites Fehmarn Belt, Dornoch Bridge and Østmarkneset, respectively. This work was supported by the Danish Ministry of Higher Education and Science through the contract "E5 Field exposure and monitoring to extend the service life of infrastructure (translation from Danish)" granted to the Danish Technological Institute (DTI).

Authors' contributions SF, MRG and HES contributed to the study conception and design. Data collection was performed by HES and SF. Data analysis was performed by SF. All authors contributed to discussing and evaluating the results. The first draft of the manuscript was written by SF and all authors commented on drafts of the manuscript. All authors read and approved the final manuscript.

Funding Open access funding provided by NTNU Norwegian University of Science and Technology (incl St. Olavs Hospital - Trondheim University Hospital).. This work was supported by the Danish Ministry of Higher Education and Science through the contract "E5 Field exposure and monitoring to extend the service life of infrastructure (translation from Danish)" granted to the Danish Technological Institute (DTI).

Code availability Not applicable.

Compliance with ethical standards

Conflict of interest Not applicable.

Availability of data and material The paper uses already published data to which references are given. Original tabulated chloride ingress data has been received from the authors to ensure accuracy. All chloride ingress data is shown graphically in the Online Resources. Data on concrete compositions and exposure conditions is given in the manuscript.

References

1. Tang L (2008) Engineering expression of the ClinConc model for prediction of free and total chloride ingress in submerged marine concrete. Cem Concr Res 38(8–9):1092–1097
2. Marchand J (2001) Modeling the behavior of unsaturated cement systems exposed to aggressive chemical environments. Mater Struct 34(4):195–200
3. Marchand J, Samson E, Maltais Y, Lee R, Sahu S (2002) Predicting the performance of concrete structures exposed to chemically aggressive environment—field validation. Mater Struct 35(10):623–631
4. fib (2006) Model code for service life design, vol fib bulletin 34. CEB-FIB
5. Collepardi M, Marcialis A, Turriziani R (1970) The kinetics of chloride ions penetration in concrete. Il Cemento 67:157–164
6. Engelund SE, Mohr L (2000) General guidelines for durability design and redesign, vol 15c. The European Union DuraCrete, New York
7. Siemes A, Edvardsen C (1999) Duracrete: service life design for concrete structures. NRC Research Press, Ottawa
8. Nilsson L, Sandberg P, Poulsen E, Tang L, Andersen A, Frederiksen JJDRDR (1997) Report no. 83: HETEK, a system for estimation of chloride ingress into concrete, theoretical background. vol 83. Danish Road Directorate
9. Poulsen E, Mejlbro L (2006) Diffusion of chloride in concrete: theory and application. Taylor & Francis, London
10. Frederiksen JM, Mejlbro L, Nilsson L-O (2008) Report TVBM-3146: fick's 2nd law-complete solutions for chloride ingress into concrete. Lund Institute of Technology, Sweden
11. Mejlbro L (1996) The complete solution of Fick's second law of diffusion with time-dependent diffusion coefficient and surface concentration. Durability of concrete in saline environment 127–158
12. Ehlen MA, III L-C (2018) Life-365^{TM} v2. 23 User's manual. Accessed 25 Feb, 2019
13. Jakobsen UH, De Weerdt K, Geiker MR (2016) Elemental zonation in marine concrete. Cement Concr Res 85:12–27
14. De Weerdt K, Orsakova D, Muller AC, Larsen CK, Pedersen B, Geiker MR (2016) Towards the understanding of chloride profiles in marine exposed concrete, impact of leaching and moisture content. Constr Build Mater 120:418–431. https://doi.org/10.1016/j.conbuildmat.2016.05.069
15. Poulsen SL, Sørensen HE (2014) Chloride ingress in old Danish bridges. In: Proceedings 2nd international congress on durability of concrete (ICDC), New Delhi, India
16. Poulsen SL, Sørensen HE, Jönsson U (2018) Chloride ingress in concrete blocks at the Rødbyhavn marine exposure site—status after 5 years. In: Paper presented at the 4th international conference on service life design for infrastructures (SLD4), Delft, The Netherlands
17. Thomas M, Matthews J (2004) Performance of pfa concrete in a marine environment—10-year results. Cement Concr Compos 26(1):5–20
18. Baroghel-Bouny V, Dierkens M, Wang X, Soive A, Saillio M, Thiery M, Thauvin B (2013) Ageing and durability of concrete in lab and in field conditions: investigation of chloride penetration. J Sustain Cement Based Mater 2(2):67–110
19. Boubitsas D, Tang L, Utgenannt P (2014) Chloride ingress in concrete exposed to marine environment-field data up to 20 years' exposure. CBI report to SBUF Project 12684
20. Skjolsvold O, Justnes H, Hammer T, Fidjestol P (2007) Long-term chloride intrusion in field-exposed concrete with and without silica fume. In: Paper presented at the Ninth CANMET/ACI international conference on Fly Ash, Silica Fume, Slag, and Natural Puzzolans in Concrete
21. Kim J, McCarter WJ, Suryanto B, Nanukuttan S, Basheer PM, Chrisp TM (2016) Chloride ingress into marine exposed concrete: a comparison of empirical-and physically-based models. Cement Concr Compos 72:133–145
22. Tang L, Boubitsas D, Utgenannt P, Abbas Z (2018) Chloride ingress and reinforcement corrosion-after 20 years' field exposure in a highway environment. RISE Research Institutes of Sweden
23. EN B (2011) 197-1: 2011. Cement, composition, specifications and conformity criteria for common cements. British Standard Institution (BSI), London

24. Lindvall A (2002) Chloride ingress in a swedish road environment: five years exposure for three concrete compositions. Chalmers tekniska högsk
25. Tang L, Utgenannt P (2007) Chloride Ingress and Reinforcement Corrosion in Concrete under De-Icing Highway Environment-A study after 10 years' field exposure, vol SP Report 2007:76. SP Technical Research Institute of Sweden,
26. DMI (2020) Danish meteorological institute. https://www.dmi.dk/vejrarkiv/. Accessed 03 Jan, 2020
27. timeanddate.com (2020) Climate & Weather Averages in Träslövsläge, Sweden. https://www.timeanddate.com/weather/@3326117/climate. Accessed 17th of Jan 2020
28. CLIMATE-DATA.ORG (2020) DORNOCH CLIMATE. https://en.climate-data.org/europe/united-kingdom/scotland/dornoch-29436/. Accessed 17th of Jan 2020
29. Andersen I (1994) Salt-og temperaturforhold i de indre danske farvande (Salt and temperature conditions in the inner Danish waters). Danish Meteorological Institute, Copenhagen, Technical Report (94–4)
30. Kim J, McCarter W, Suryanto B, Nanukuttan S, Basheer P, Chrisp TJC, C (2016) Chloride ingress into marine exposed concrete: A comparison of empirical-and physically-based models. Cem Concr Compos 72:133–145
31. CLIMATE-DATA.ORG (2020) BORÅS CLIMATE. https://en.climate-data.org/europe/sweden/vaestra-goetalands-laen/boras-6325/. Accessed 17th of Jan 2020
32. Poulsen SL (2018) Chloride ingress in concrete blocks at the Rødbyhavn marine exposure site—status after 5 years. In: 4th International conference on service life design for infrastructures (SLD4). Delft, The Netherlands
33. Tang L (1996) Electrically accelerated methods for determining chloride diffusivity in concrete—current development. Mag Concr Res 48(176):173–179
34. De Weerdt K, Orsáková D, Müller AC, Larsen CK, Pedersen B, Geiker MR (2016) Towards the understanding of chloride profiles in marine exposed concrete, impact of leaching and moisture content. Constr Build Mater 120:418–431
35. Angst UM, Geiker MR, Alonso MC, Polder R, Isgor OB, Elsener B, Wong H, Michel A, Hornbostel K, Gehlen C (2019) The effect of the steel–concrete interface on chloride-induced corrosion initiation in concrete: a critical review by RILEM TC 262-SCI. Mater Struct 52(4):88
36. Angst U, Elsener B, Larsen CK, Vennesland Ø (2009) Critical chloride content in reinforced concrete—a review. Cem Concr Res 39(12):1122–1138. https://doi.org/10.1016/j.cemconres.2009.08.006
37. Justnes H, Geiker M (2012) A critical view on service life predictions based on chloride induced corrosion. Proc MicroDurability
38. Reddy ARA, Agarwal A, Pillai RG (2013) Service life prediction models for concrete structures—a comparative study. In: Rehabilitation and restoration of structures and advances in building sciences. Chennai, India
39. Olsson N, Wahid FA, Nilsson L-O, Thiel C, Wong HS, Baroghel-Bouny V (2018) Wick action in mature mortars with binary cements containing slag or silica fume–The relation between chloride and moisture transport properties under non-saturated conditions. Cem Concr Res 111:94–103
40. Michel A (2013) Reinforcement corrosion: numerical simulation and service life prediction. Technical University of Denmark, Lyngby
41. Hemstad P, Machner A, De Weerdt K (2020) The effect of artificial leaching with HCl on chloride binding in ordinary Portland cement paste. Cem Concr Res 130:105976
42. Olsson N, Lothenbach B, Baroghel-Bouny V, Nilsson L-O (2018) Unsaturated ion diffusion in cementitious materials—the effect of slag and silica fume. Cem Concr Res 108:31–37
43. Flint M, Michel A, Billington S, Geiker MR (2014) Influence of temporal resolution and processing of exposure data on modeling of chloride ingress and reinforcement corrosion in concrete. Mater Struct 47(4):729–748